J. Biochem. **123**, 1104-1111 (1998)

Fluorescence Resonance Energy Transfer between Points on Tropomyosin and Actin in Skeletal Muscle Thin Filaments: Does Tropomyosin Move?[1]

Masao Miki,*[,2] Tomoo Miura,* Ken-Ichi Sano,† Hiroyuki Kimura,* Hiroyuki Kondo,* Hiroshi Ishida,* and Yuichiro Maéda†

**Department of Applied Chemistry and BioTechnology, Fukui University, 3-9-1 Bunkyo, Fukui 910-8507; and †International Institute for Advanced Research, Matsushita Electric Industrial Co., Ltd., 3-4 Hikaridai, Seika 619-02*

Received for publication, December 9, 1997

Fluorescence resonance energy transfer (FRET) spectroscopy has been used to determine spatial relationships between residues on tropomyosin and actin in reconstituted muscle thin filament, and to detect a positional change of tropomyosin relative to actin on the thin filament in the presence and absence of Ca^{2+} ions. In addition to Cys-190 which is a single cysteine residue in rabbit skeletal muscle α-tropomyosin, a new site, Cys-87 which is a unique cysteine residue in a mutant α-tropomyosin, was labeled with a resonance energy donor molecule, 5-(2-iodoacetylaminoethyl)aminonaphthalene 1-sulfonic acid (IAED-ANS). On the other hand, Gln-41, Lys-61, Cys-374, and the ATP-binding site of actin were selectively labeled with acceptor probes: fluorescein cadaverine, fluorescein 5-isothiocyanate, 4-dimethyl-aminophenylazophenyl 4′-maleimide, and TNP-ATP (or TNP-ADP), respectively. The distances between probes attached to position 87 of the mutant tropomyosin and Gln-41, Lys-61, Cys-374, or the nucleotide-binding site of actin on the reconstituted thin filament in the presence of Ca^{2+} ion were measured to be 43.2, 49.7, 45.4, and 35.2 Å, respectively, and the distance between probes attached to position 190 of tropomyosin and Gln-41 or the nucleotide-binding site of actin were 51.6 and 43.1 Å, respectively. The transfer efficiencies between these donor and acceptor molecules were large, so that the efficiency should be very sensitive to changes in distance between probes attached to tropomyosin and actin. However, the transfer efficiency did not change appreciably upon removal of Ca^{2+} ions, suggesting that tropomyosin does not change its position on the reconstituted thin filament in response to a change in Ca^{2+} ion concentration. The present results do not support the notion of tropomyosin movement on skeletal muscle thin filaments as proposed in the steric blocking theory.

Key words: actin, FRET, skeletal muscle regulation, steric blocking theory, tropomyosin.

In striated muscle, the interaction of myosin with actin is regulated by tropomyosin (Tm) and troponin (Tn) on actin filaments in response to a change in Ca^{2+} concentration from approximately 10^{-7} to 10^{-5} M (*1*). Tn is a complex of three proteins: troponin C (TnC), troponin I (TnI), and troponin T (TnT). The binding of Ca^{2+} to TnC induces a conformational change in Tn, which is propagated along the actin filament by Tm. The mechanism of this regulatory process is still not well understood. X-Ray diffraction studies of muscle showed a significant change in the layer line intensities depending on whether the muscle is in a relaxed or contracting state. This intensity change has been interpreted in terms of an azimuthal shift of the Tm strands in the grooves of the actin helix. Based on this interpretation, the steric blocking theory has been proposed, in which Tm sterically blocks the myosin-binding site on the thin filament during relaxation (*2, 3*). Although widely accepted, the steric blocking model has not been confirmed. Using the known atomic structure of the actin molecule (*4*), analysis of the low-angle X-ray diffraction and three-dimensional reconstruction by electron microscopy have been employed in attempts to demonstrate Tm movement (*5, 6*).

Fluorescence resonance energy transfer has also been employed in several attempts to detect movement of Tm on the reconstituted thin filament. Tropomyosin has a two-stranded α-helical coiled coil structure. Rabbit skeletal muscle Tm consists of equimolar α-α and α-β hetero-

[1] This work was partially supported by a Grant-in-Aid for Scientific Research from the Ministry of Education, Science, Sports and Culture of Japan.

[2] To whom correspondence should be addressed. Tel: +81-776-27-8786, Fax: +81-776-27-8747, E-mail: masao@acbio.fukui-u.ac.jp

Abbreviations: DABMI, 4-dimethylaminophenylazophenyl 4′-maleimide; DTT, dithiothreitol; EGTA, ethylene glycol-bis(2-aminoethyl ether)-*N,N,N′,N′*-tetraacetic acid; FITC, fluorescein 5-isothiocyanate; FLC, fluorescein cadaverine; FRET, fluorescence resonance energy transfer; IAEDANS, 5-(2-iodoacetylaminoethyl)aminonaphthalene 1-sulfonic acid; TNP-ADP, 2′(or 3′)-*O*-(2,4,6-trinitrophenyl)-adenosine 5′-diphosphate; Tm, tropomyosin; mTm, mutant tropomyosin; Tn, troponin.

dimers. The α-chain contains a single cysteine (Cys-190) that can be modified without greatly altering the biological activity, depending on the reagent. Thus, Cys-190 was labeled with a fluorescence donor and Cys-374, the nucleotide-binding site, or Lys-61 on actin was labeled with the acceptor, and fluorescence resonance energy transfer between these sites was measured in the presence and absence of Ca^{2+} ions (*7, 8*). However, the transfer efficiency between a Tm-bound donor and an actin-bound acceptor on the reconstituted thin filament was not as sensitive to the Ca^{2+} concentration as expected from the steric blocking theory. Until now, Cys-190 has served as the major structural probe for Tm. In the present study, a mutant of rabbit skeletal muscle α-α-Tm was expressed in *Escherichia coli*, in which two residues were replaced (Ser-87-Cys; Cys-190-Ile) and three additional residues M-A-S- were inserted at the N-terminus in order to restore the binding ability to F-actin according to Monteiro *et al.* (*9*). The new site (Cys-87) of the mutant Tm (mTm) was labeled with a fluorescence energy donor, 5-(2-iodoacetylaminoethyl)-aminonaphthalene-1-sulfonic acid (IAEDANS). On the other hand, Gln-41, Lys-61, Cys-374, or the nucleotide-binding site on actin was labeled with acceptors: fluorescein cadaverine (FLC), fluorescein 5-isothiocyanate (FITC), 4-dimethylaminophenylazophenyl 4′-maleimide (DABMI), or 2′(or 3′)-*O*-(2,4,6-trinitrophenyl)adenosine 5′-diphosphate (TNP-ADP), respectively. The resonance energy transfer efficiency between these probes was high, and therefore should be very sensitive to changes in the distance between the Tm-bound donor and the actin-bound acceptor. Using these donor-acceptor pairs, Tm movement on the reconstituted thin filament has been tested under various conditions.

MATERIALS AND METHODS

Reagents—Phalloidin from *Amanita phalloides* was purchased from Boehringer Mannheim Biochemica. TNP-ATP was synthesized according to the method of Hiratsuka and Uchida (*10*). FITC was purchased from Sigma Chemical. IAEDANS, DABMI, and FLC were from Molecular Probes. BCA protein assay reagent was from Pierce Chemicals. All other chemicals were analytical grade.

Protein Preparations—Actin, S1, and troponin from rabbit skeletal muscle were prepared as described in a previous report (*8*). Cardiac Tm was prepared from rabbit hearts as previously reported (*8*). Rabbit cardiac Tm has the same amino acid sequence as rabbit skeletal α-Tm peptide, which contains a single cysteine at position 190 (*11*). Microbial transglutaminase was a generous gift from Food Research and Development Laboratories, Ajinomoto. In contrast to transglutaminase from guinea pigs, this enzyme does not require Ca^{2+} for its activity (*12, 13*). The following extinction coefficients were used to calculate protein concentrations: $A_{290nm}=0.63$ $(mg/ml)^{-1}\cdot cm^{-1}$ for G-actin, and $A_{280nm}=0.75$ for S1, 0.33 for Tm, and 0.45 $(mg/ml)^{-1}\cdot cm^{-1}$ for Tn. Concentrations of labeled proteins and transglutaminase were measured with the Pierce BCA protein assay reagent. Relative molecular masses of 42,000 for actin, 115,000 for S1, 66,000 for Tm, 69,000 for Tn, and 38,000 for microbial transglutaminase were used.

Preparation of Fusion MAS-Tm (S87C,C190I)—Expression vector of fusion MASTm(S87C,C190) was constructed as follows. Firstly, wild-type α-Tm in M13 (*14*) was mutagenized by single-stranded site-directed mutagenesis (Amersham, Sculptor *in vitro* mutagenesis system) to mutate serine 87 to cysteine and cysteine 190 to isoleucine. Secondly, a *Pst*I site was introduced at the N-terminal region of Tm (S87C,C190I) by single-stranded site-directed mutagenesis as described above. Thirdly, the *Pst*I–*Bam*HI fragment of Tm (S87C,C190I) was ligated to both the annealed oligonucleotides which contain the N-terminal sequence of Tm with additional MAS sequence and pET3d which was digested by *Nco*I and *Bam*HI. The DNA sequence of MASTm (S87C,C190I) in the expression vector was confirmed by dideoxy sequencing using the autoread sequencer (Pharmacia LKB ALFII). Expression in *E. coli* and purification of expressed MASTm (S87,C190I) were carried out according to Kluwe *et al.* (*14*) and Miegel *et al.* (*15*), respectively.

Labeling of Proteins—Labeling of actin at Lys-61 with FITC, or at Cys-374 with DABMI was carried out as previously reported (*7, 8*). Labeling of actin at Gln-41 with FLC or at the nucleotide-binding site with TNP-ADP was carried out as mentioned in the previous paper (*16*). Labeling of Tm at Cys-190 with IAEDANS was carried out as previously reported (*8*). Labeling of mutant Tm at Cys-87 with IAEDANS was carried out as follows. Tropomyosin at a concentration of 1 mg/ml was incubated with a twentyfold molar excess of IAEDANS in a buffer solution containing 40 mM phosphate buffer (pH 7.0), 1 mM EDTA, and 1 M KCl for 24 h at 25°C. The reaction was terminated by the addition of 1 mM DTT, and labeled mTm was precipitated by centrifugation with 66% saturated ammonium sulfate at $10,000\times g$ for 20 min in order to remove unreacted dye. The pellet was dissolved in 2 mM phosphate buffer (pH 7.0) and 0.2 mM DTT, and dialyzed exhaustively against the same solution. The absorption coefficients of 26,400 $M^{-1}\cdot cm^{-1}$ at 408 nm for TNP-ADP (*10*), 24,800 $M^{-1}\cdot cm^{-1}$ at 460 nm for DABMI (*7*), 75,500 $M^{-1}\cdot cm^{-1}$ at 493 nm for FLC (*17*), 74,500 $M^{-1}\cdot cm^{-1}$ at 493 nm for FITC (*18*), and 6,100 $M^{-1}\cdot cm^{-1}$ at 337 nm for IAEDANS (*19*) were used for the determination of the labeling ratios. Typical labeling ratios were 0.60 ± 0.1 for TNP-ADP to actin, 0.71 for FLC to actin, 1.0 for FITC to actin, 1.0 for DABMI to actin, 1.60 for AEDANS to Tm, 1.20 for AEDANS to mutant Tm.

Spectroscopic Measurements—Absorption was measured with a Hitachi U2000 spectrophotometer. Steady-state fluorescence was measured with a Hitachi 850 fluorometer. Sample cells were placed in a thermostated cell holder. Steady-state fluorescence polarization measurements were carried out on the AEDANS-Tm in the presence of various concentrations of sucrose at 20°C to measure the limiting anisotropy of AEDANS-Tm as previously mentioned (*20*).

Fluorescence Resonance Energy Transfer—The efficiency, E, of resonance energy transfer between probes was determined by measuring the fluorescence intensity of the donor in the presence (F_{DA}) and absence (F_{D0}) of the acceptor and is given by

$$E=1-F_{DA}/F_{D0} \quad (1)$$

From the absorptions of the samples at the excitation (A_{ex}) and emission (A_{em}) wavelengths, the decrease of the fluorescence intensity due to inner filter effects was corrected, using Eq. 2, as previously reported (*8*).

$$F_{corr} = F_{obs} \times 10^{(Aex+Aem)/2} \quad (2)$$

According to Förster's theory [see reviews: Stryer (*21*), and Lakowicz (*22*)], the efficiency is related to the distance (R) between probes and Förster's critical distance (R_0) at which the transfer efficiency is equal to 50% by

$$E = R_0^6/(R_0^6 + R^6) \quad (3)$$

R_0 (in nm) is given by the equation

$$R_0^6 = (8.79 \times 10^{-11}) n^{-4} \kappa^2 Q_{D0} J \quad (4)$$

where n is the refractive index of the medium, taken to be 1.4, κ^2 is the orientation factor; Q_{D0} is the quantum yield of the donor in the absence of the acceptor; and J is the spectral overlap integral (in $M^{-1} \cdot cm^{-1} \cdot nm^4$) between the donor emission $F_D(\lambda)$ and acceptor absorption $\varepsilon_A(\lambda)$ spectra, defined by

$$J = \int F_D(\lambda) \varepsilon_A(\lambda) \lambda^4 d\lambda \Big/ \int F_D(\lambda) d\lambda \quad (5)$$

The quantum yield of AEDANS-Tm in 10 mM phosphate buffer at pH 7.0 was 0.29, as previously reported (*8*). It was not changed by the addition of F-actin and troponin. The quantum yield of AEDANS-mTm was determined to be 0.41 by comparing the emission spectrum with that of AEDANS-Tm. It was increased to 0.46 by the addition of F-actin and further increased to 0.47 by the addition of F-actin and Tn, but did not change depending on the Ca^{2+} concentration. κ^2 was taken as 2/3 for calculation of distances, and the maximum and minimum values of κ^2 were estimated by the method of Dale *et al.* (*23*).

Other Methods—SDS-PAGE (3% stacking gel and 7-18% gradient separation gel) was carried out according to Laemmli (*24*). ATPase activity was measured by the method of Tausky and Shorr (*25*). The biological activity of the labeled Tm was assayed by determining the Ca^{2+}-dependent regulation of actoS1 ATPase in a fully reconstituted system. Measurements were performed at 25°C in 10 mM KCl, 4 mM $MgCl_2$, 2.0 mM ATP, 20 mM Tris-HCl (pH 7.6), 0.5 mM DTT, and 50 μM $CaCl_2$ (+Ca state) or 2 mM EGTA (−Ca state). Protein concentrations were: 1 mg/ml F-actin, 0.33 mg/ml Tm, 0.35 mg/ml Tn, and 0.06 mg/ml S1.

RESULTS

In this work, the AEDANS moiety bound to Cys-190 of Tm or Cys-87 of mTm was used as the energy-transfer donor, while FLC, FITC, DABMI, or TNP-ADP bound to Gln-41, Lys-61, Cys-374, or the nucleotide-binding site respectively in F-actin was used as the energy-transfer acceptor. The absorption spectra of the energy-transfer acceptors bound to actin overlap well with the fluorescence emission spectrum of AEDANS bound to Tm (Cys-190 and Cys-87). To test whether the labeled Tm retains the essential property of being able to participate in the calcium regulation process, the ATPase activities of reconstituted systems composed of S1, Tn, Tm, and F-actin were measured in the presence and absence of Ca^{2+}. The regulatory capacity value is defined as $1-(Act_{EGTA}/Act_{Ca^{2+}})$, where $Act_{Ca^{2+}}$ and Act_{EGTA} are the Mg-ATPase activities in the presence and absence of Ca^{2+}, respectively. The values of FA/Tm/Tn, FA/Cys-190-labeled-Tm/Tn, and FA/Cys-87-labeled-mTm/Tn were 0.80, 0.75, and 0.71, respectively. The results showed that the modification at Cys-190 on Tm or at Cys-87 on mTm with IAEDANS does not impair the ability of Tm to regulate the acto-S1 ATPase activity in conjunction with Tn and Ca^{2+}. Tao *et al.* (*7*) reported that the ATPase activity of reconstituted systems composed of S1, Tn, Cys-190-labled-Tm, and DABMI- or TNP-ADP-labeled-F-actin exhibited marked Ca^{2+} sensitivity. We confirmed their results. Further the ATPase activities of reconstituted systems composed of S1, Tn, Cys-190-labeled-Tm or Cys-87-labeled-mTm, and FLC-, FITC, DABMI-, or TNP-ADP-labeled-F-actin were measured in the presence and absence of Ca^{2+}. In all cases, the ATPase activity composed of the energy-transfer donor-labeled-Tm and the acceptor-labeled-actin exhibited strong Ca^{2+} sensitivity (the regulatory capacity values are 0.8-0.7). The results showed that the energy donor-labeled Tm and acceptor-labeled actin which were used for FRET measurements in the present studies retain their essential properties, being able to participate in the calcium regulation process.

FRET between Cys-87 of mTm and the Nucleotide-Binding Site, Cys-374, Lys-61, or Gln-41 of Actin in a Reconstituted Thin Filament—The fluorescence spectrum of AEDANS bound to Cys-87 of mTm has the emission maximum at 495 nm in 30 mM KCl, 2 mM $MgCl_2$, 20 mM Tris-HCl (pH 7.6), and 1 mM NaN_3 (buffer F). Upon the addition of F-actin, the emission peak was blue-shifted by 5 nm, and the fluorescence intensity increased by 12%. Upon further addition of troponin the fluorescence intensity slightly increased by 2% without any shift of the emission peak. The overlap integral J was calculated to be 6.98×10^{14} $M^{-1} \cdot cm^{-1} \cdot nm^4$ for AEDANS-TNP-ADP, 5.76×10^{14} $M^{-1} \cdot cm^{-1} \cdot nm^4$ for AEDANS-DABMI, 15.22×10^{14} $M^{-1} \cdot cm^{-1} \cdot nm^4$ for AEDANS-FITC, and 15.41×10^{14} $M^{-1} \cdot cm^{-1} \cdot nm^4$ for AEDANS-FLC. By taking $n = 1.4$, $\kappa^2 = 2/3$, and $Q_0 = 0.47$, Förster's critical distance R_0 was calculated to be 41.4 Å for AEDANS-TNP-ADP, 40.0 Å for AEDANS-DABMI, 47.1 Å for AEDANS-FITC, and 47.2 Å for AEDANS-FLC.

The fluorescence spectra of AEDANS bound to Cys-87 of mTm on the reconstituted thin filament in the absence and presence of acceptor (TNP-ADP) were measured in buffer F and 50 μM $CaCl_2$ (+Ca state). Figure 1 shows that the donor fluorescence (AEDANS-mTm) was significantly quenched in the presence of acceptor owing to energy transfer. Removal of free Ca^{2+} ions in the sample solution by the addition of 2 mM EGTA did not change the spectra of AEDANS-mTm/Tn/F-actin in the presence and absence of acceptor (TNP-ADP). This result indicates that the distance between probes attached to Cys-87 of mTm and the nucleotide-binding site of actin does not change when Ca^{2+} ions are removed from Tn.

To obtain more quantitative data on the transfer efficiency, the ratio of donor fluorescence quenching was measured by titrating AEDANS-mTm/Tn with TNP-ADP-F-actin in the presence of Ca^{2+} (buffer F + 50 μM $CaCl_2$) or in the absence of Ca^{2+} (buffer F + 2 mM EGTA). The fluorescence intensity of AEDANS-mTm was measured at 490 nm. For the correction of the fluorescence intensity change upon binding to actin filaments or due to dilution effects, the same amount of non-labeled F-actin was added to the AEDANS-mTm/Tn solution, and the ratio of the fluorescence intensities was taken. The apparent decrease

of the fluorescence intensity due to the inner filter effects arising from the absorbance of TNP-ADP-F-actin was corrected according to Eq. 2. The fluorescence ratio decreased rapidly in the range of actin/Tm molar ratio up to 3, then gradually decreased up to 7, and became almost constant in the range over 7 (Fig. 2). The results suggest that the energy transfer occurs through a specific interaction between actin and Tm. From the saturation points, the apparent transfer efficiency was taken to be 0.49 for both +Ca state and −Ca state. Taking into account the labeling ratio of TNP-ADP to actin being 0.67, the transfer efficiency was calculated to be 0.72, which corresponds to the distance of 35.2 Å, assuming that the energy transfer occurs between a single donor and a single acceptor.

Since DABMI is non-fluorescent, like TNP-ADP, under our present experimental conditions, FRET measurements between AEDANS-mTm and DABMI-F-actin were carried out under the same conditions as in the case of TNP-ADP-F-actin. The fluorescence spectrum of AEDANS-mTm on the reconstituted thin filament was significantly quenched in the presence of acceptor (DABMI-F-actin), but removal of free Ca^{2+} ions in the sample solution did not change the spectra of AEDANS-mTm in the absence and presence of acceptor. The ratio of donor fluorescence quenching was measured by titrating AEDANS-mTm with DABMI-F-actin under the same experimental conditions as used for TNP-ADP-F-actin. The ratio decreased in the same way as the case of TNP-ADP-F-actin as the molar ratio of actin to Tm was increased. The extent of decrease did not change whether Ca^{2+} ions were present or not. From the saturation level, the transfer efficiency was determined to be 0.32, which corresponds to the distance of 45.4 Å.

FITC-actin was polymerized in 30 mM KCl, 2 mM $MgCl_2$, 20 mM Tris-HCl (pH 7.6), 0.1 mM ATP, and 1 mM NaN_3 (buffer A) in the presence of a twofold molar excess of phalloidin, as previously reported (*8, 19*). The fluorescence spectra of (i) F-actin/AEDANS-mTm/Tn, (ii) FITC-F-actin/mTm/Tn, and (iii) FITC-F-actin/AEDANS-mTm/Tn were measured in buffer A+50 μM $CaCl_2$ at 20°C (Fig. 3). The excitation wavelength was 340 nm. The fluorescence intensity of FITC-F-actin/AEDANS-mTm/Tn at wavelengths shorter than 480 nm was substantially quenched compared with that of F-actin/AEDANS-mTm/Tn (in the absence of acceptor). This can be attributed mainly to the resonance energy transfer from AEDANS-Tm to FITC-F-actin.

To obtain more quantitative data on the transfer efficiency, the ratio of donor fluorescence quenching was measured by titrating AEDANS-mTm/Tn with FITC-F-actin in the presence (buffer A+50 μM $CaCl_2$) or absence (buffer A+2 mM EGTA) of Ca^{2+} ions. The fluorescence intensity was measured at 460 nm, where no contribution from the fluorescence of FITC occurs (Fig. 3). The inner

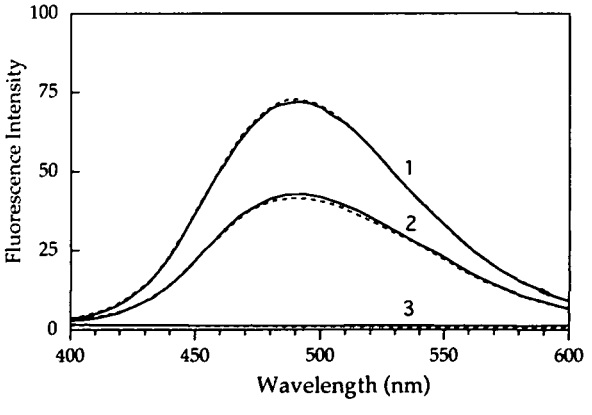

Fig. 1. **Fluorescence spectra of AEDANS bound to Cys-87 of mTm on the reconstituted thin filament in the presence and absence of acceptor (TNP-ADP).** (1) F-actin/AEDANS-Tm/Tn/± Ca, (2) TNP-ADP-F-actin/AEDANS-Tm/Tn/±Ca, (3) TNP-ADP-F-actin/Tm/Tn/±Ca. Spectra were measured at 20°C in 30 mM KCl, 2 mM $MgCl_2$, 20 mM Tris-HCl (pH 7.6), 1 mM NaN_3 (buffer F), and 50 μM $CaCl_2$ (+Ca; solid lines) or 2 mM EGTA (−Ca; broken lines). Concentrations of actin, mTm, and Tn were 0.2, 0.045, and 0.047 mg/ml, respectively. Excitation was at 340 nm.

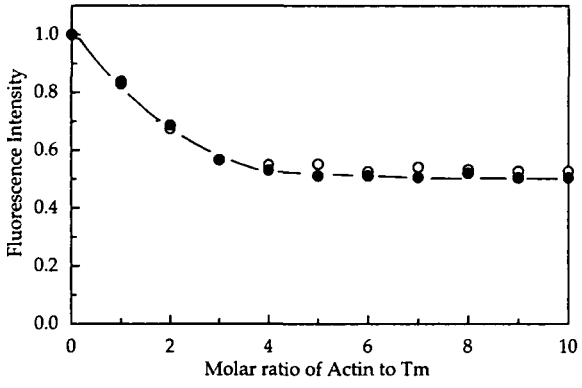

Fig. 2. **Relative fluorescence intensities of AEDANS bound to Cys-87 of mTm in the Tn-Tm complex *vs.* molar ratio of TNP-ADP-F-actin.** Values were obtained in buffer F and 50 μM $CaCl_2$ (closed circles) or 2 mM EGTA (open circles) at 20°C, after correction of the inner filter effects according to Eq. 2. Concentrations of AEDANS-mTm and Tn were 0.045 and 0.047 mg/ml, respectively. Excitation was at 340 nm and emission was measured at 490 nm.

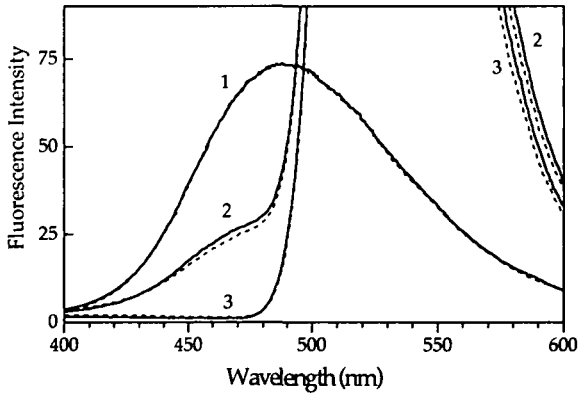

Fig. 3. **Fluorescence spectra of AEDANS bound to Cys-87 of mTm on the reconstituted thin filament in the presence and absence of acceptor (FITC).** (1) F-actin/AEDANS-mTm/Tn, (2) FITC-F-actin/AEDANS-mTm/Tn, (3) FITC-F-actin/Tm/Tn. Spectra were measured at 20°C in 30 mM KCl, 2 mM $MgCl_2$, 20 mM Tris-HCl (pH 7.6), 1 mM NaN_3, 0.1 mM ATP (buffer A), and 50 μM $CaCl_2$ (+Ca; solid lines) or 2 mM EGTA (−Ca; broken lines). Concentrations of actin, mTm, and Tn were 0.2, 0.045, and 0.047 mg/ml, respectively. Excitation was at 340 nm. The fluorescence spectra of 2 and 3 at wavelengths from ~495 to ~575 nm, which derive mainly from FITC with an emission peak at 520 nm, are omitted from the figure.

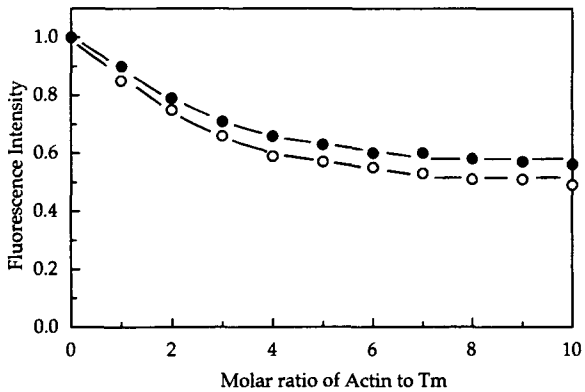

Fig. 4. **Relative fluorescence intensities of AEDANS bound to Cys-87 of mTm in the Tn-Tm complex *vs.* molar ratio of FITC-F-actin.** Values were obtained in buffer A and 50 μM $CaCl_2$ (closed circles) or 2 mM EGTA (open circles) at 20°C, after correction of the inner filter effects. Concentrations of Tn and AEDANS-mTm were 0.047 and 0.045 mg/ml, respectively. Excitation was at 340 nm and emission was measured at 460 nm.

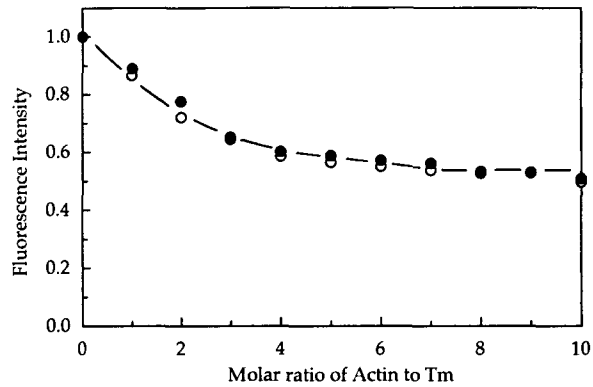

Fig. 5. **Relative fluorescence intensities of AEDANS bound to Cys-87 of mTm in the Tn-Tm complex *vs.* molar ratio of FLC-F-actin.** Values were obtained in buffer A and 50 μM $CaCl_2$ (closed circles) or 2 mM EGTA (open circles) at 20°C, after correction of the inner filter effects. Concentrations of Tn and AEDANS-mTm were 0.047 and 0.045 mg/ml, respectively. Excitation was at 340 nm and emission was measured at 460 nm.

filter effects due to the absorbance of FITC-F-actin were corrected according to Eq. 2. The fluorescence intensity decreased rapidly in the range of actin/Tm molar ratio up to 3, then gradually decreased up to 7, and saturated over 7 in the same way as in the case of AEDANS-Tm and TNP-ADP-F-actin (Fig. 4). In this case, the extent of the decrease slightly depends on the Ca^{2+} concentration. The transfer efficiency was calculated to be 0.42 in the presence of Ca^{2+} and 0.49 in the absence of Ca^{2+}, which correspond to distances of 49.7 and 47.4 Å, respectively.

FLC-G-actin was polymerized in buffer A in the presence of a twofold molar excess of phalloidin in order to prevent the depolymerization of FLC-actin. Since FLC has the same fluorophore moiety as FITC, FRET measurements were carried out under the same experimental conditions as in the case of FITC-F-actin. The ratio of donor fluorescence quenching was measured by titrating AEDANS-mTm/Tn with FLC-F-actin in buffer A in the presence or absence of Ca^{2+} ions. The fluorescence intensity was measured at 460 nm where no contribution from the fluorescence of FLC occurs. The fluorescence intensity decreased as the molar ratio of actin to Tm increased, in the same way as the case of FLC-F-actin (Fig. 5). The transfer efficiency was determined to be 0.45 both in +Ca and −Ca states. Taking into account the labeling ratio of FLC to actin of 0.71, the transfer efficiency was calculated to be 0.63 both in +Ca and −Ca states. The efficiency corresponds to the distance of 43.0 Å, assuming that the transfer occurs between a single donor and a single acceptor.

FRET between Cys-190 on Tm and the Nucleotide-Binding Site or Gln-41 on Actin in a Reconstituted Thin Filament—The fluorescence spectrum of AEDANS bound to Cys-190 of Tm has the emission maximum at 495 nm and is not changed by binding to F-actin or to F-actin/Tn in the presence or absence of Ca^{2+}. The overlap integral J was calculated to be 6.81×10^{14} $M^{-1}\cdot cm^{-1}\cdot nm^4$ for AEDANS-TNP-ADP and 14.31×10^{14} $M^{-1}\cdot cm^{-1}\cdot nm^4$ for AEDANS-FLC. By taking $n=1.4$, $\kappa^2=2/3$ and $Q_0=0.29$ (*8*), the Förster's critical distance R_0 was calculated to be 38.0 Å for AEDANS-TNP-ADP and 43.0 Å for AEDANS-FLC.

The fluorescence spectra of AEDANS bound to Cys-190 of Tm on the reconstituted thin filament in the absence and presence of acceptor (TNP-ADP) were measured under the same solvent conditions as in the case of mutant Tm. The results showed that the donor fluorescence (AEDANS-Tm) was strongly quenched in the presence of acceptor (TNP-ADP) owing to energy transfer. Removal of free Ca^{2+} ions in the sample solution by the addition of 2 mM EGTA did not change the spectra. As described in the case of mutant Tm, the ratio of donor fluorescence quenching was measured by titrating AEDANS-Tm/Tn with TNP-ADP-F-actin in the presence of Ca^{2+} (buffer F+50 μM $CaCl_2$) or in the absence of Ca^{2+} (buffer F+2 mM EGTA). The fluorescence ratio decreased rapidly in the range of actin/Tm molar ratio up to 3, then gradually decreased up to 7, and saturated over 7. From the saturation points, the apparent transfer efficiency was taken to be 0.21 ± 0.03 for both the +Ca state and −Ca state. Taking into account the labeling ratio of TNP-ADP to actin being 0.67, the transfer efficiency was calculated to be 0.32 ± 0.04 which corresponds to the distance of 43.1 ± 1.4 Å. The ratio of donor quenching was also measured using FLC-F-actin as the acceptor in the presence or absence of Ca^{2+}. The fluorescence intensity of the donor was measured at 460 nm to avoid emission from the acceptor molecule, FLC. The apparent transfer efficiency was 0.18 ± 0.03 for both the +Ca and −Ca states. Taking into account the labeling ratio of FLC to actin of 0.71, the transfer efficiency was calculated to be 0.25 ± 0.04, which corresponds to the distance of 51.6 ± 2.0 Å in the +Ca and −Ca states.

DISCUSSION

The fluorescence emission spectrum of AEDANS bound to Cys-190 of Tm did not change upon addition of F-actin and/or Tn in the presence or absence of Ca^{2+} ions. Different probes attached to Cys-190 on Tm are also insensitive to actin binding (*26*), which suggests that the region around Cys-190 does not interact directly with actin. However the emission spectrum of AEDANS bound to Cys-87 of mTm is significantly sensitive to actin and/or troponin binding. The subunit of Tm consists of repeating seven-residue units

(abcdefg) and the coiled-coil structure is stabilized by both hydrophobic interaction between the regular nonpolar side chains (positions a and d) and electrostatic interactions between the regular charged side chains. Cys-190 is at the position of a, which is located in the contact region between two subunits, and Cys-87 is at position of c, which is exposed to the solvent. Electron microscopic studies revealed the troponin complex on Tm as a globular mass near Cys-190 of Tm, composed primarily of TnC and TnI, with a rodlike tail, which is TnT, extending toward the carboxyl terminus of Tm [for review, see Zot and Potter (*27*)]. Cys-190 is close to, and Cys-87 is far from the troponin-binding site, but the effect of Tn binding on the fluorescence spectrum was observed only in the case of Cys-87. The results suggest that the side chain of Cys-87 directly interacts with the actin surface, and the binding of Tn strengthens the interaction.

The fluorescence intensities of donor-labeled Tm titrated with the acceptor-labeled F-actin (in Figs. 2, 4, and 5) decreased biphasically, *i.e.*, rapidly decreased up to an actin/Tm molar ratio of 3, then gradually decreased up to the molar ratio of 7 and became almost constant over 7. On skeletal muscle thin filaments, one Tm covers seven actin monomers. An electron microscopic study revealed that the binding mode of Tm to F-actin at high molar ratios differs from that at low molar ratios of actin to Tm (*28*). A quasielastic light scattering study *in vitro* showed that extra Tm can bind to F-actin up to twice the molar ratio seen *in vivo* under physiological salt conditions (*29*). At low molar ratios of actin to Tm, extra Tm may bind to actin, resulting in extra resonance energy transfer between probes on Tm and F-actin. However, in the range of molar ratio of actin to Tm over 7, the transfer efficiency is constant, which suggests that the energy transfer occurs through a specific interaction between actin and Tm under physiological conditions.

In the present analysis of FRET data, a single donor-acceptor pair was assumed. As previously reported (*16*), even in the case of a single donor and multiple acceptors in a reconstituted thin filament, the present analysis gives a nearest-neighbor distance without a large error. Since Tm is a dimer of α-chains, the energy donor molecule, AEDANS, binds to Tm at a ratio of more than 1 (mol/mol). In the case of two donors and one acceptor, FRET occurs from one donor to one acceptor and from the other donor to the same acceptor. If their distances are the same, the analysis of the distance is the same as in the case of a single donor-acceptor pair. Two α-chains in Tm associate in register in a coiled-coil fashion, so the two donors in Tm should be located very close to each other. The present analysis of distance gives the average of two distances between two donors on α_1- or α_2-chains of Tm and one acceptor on F-actin.

In calculation of the distances between probes, the value of 2/3 was used for the orientation factor, which corresponds to the case where both donor and acceptor molecules rotate rapidly. Theoretically κ^2 varies over 0-4, and in most cases is not known accurately. The upper and lower bounds of this parameter were calculated by the method of Dale *et al.* (*23*). The limiting anisotropies of FLC bound to Gln-41 and FITC bound to Lys-61 of actin were previously reported to be 0.217 (*30*) and 0.273 (*20*), respectively, and those of AEDANS bound to Cys-190 of Tm or Cys-87 of mTm were determined in this study to be 0.091 and 0.117, respectively from the steady-state fluorescence polarization measurements in the presence of various concentrations of sucrose at 20°C. The fundamental anisotropies of AEDANS, FLC, and FITC were previously reported to be 0.376 (*30*), 0.341 (*30*), and 0.376 (*31*), respectively. These values give a maximum error range for the critical distance (R_0) calculated by using $\kappa^2=2/3$ of ~25%, *i.e.*, the calculated range appears to be unacceptably large. However, it should be noted here that the maximum and minimum values correspond to the case where the axis of the cone in which the donor and acceptor transition moments rotate rapidly along unique directions (*i.e.* perpendicular or parallel). Usually, proteins are very flexible macromolecules. Then, the directions of the transition moments of probes should be randomized due to segmental motions. Therefore, the true range of κ^2 is much narrower. Indeed, we have pointed out that reasonable agreement was obtained between intra- and inter-molecular distances in G-actin and F-actin determined by FRET assuming $\kappa^2=2/3$ and the distances determined from X-ray diffraction data (*32, 33*).

The distances between probes attached to Tm and actin in the reconstituted thin filament determined in the present study are summarized in Table I. Tao *et al.* (*7*) previously reported that the distance between Cys-190 of Tm and Cys-374 or the nucleotide-binding site of actin in the reconstituted thin filament did not change upon the binding of Ca^{2+} to Tn. They suggested that the Tm-bound donor and the actin-bound acceptors can be located relative to each other so that the movement of Tm with respect to the grooves of actin produces no net change in the extent of energy transfer. However, such acceptor locations are restricted to a narrow area. Later, the distance between Cys-190 of Tm and Lys-61 of actin was measured in the presence and absence of Ca^{2+} ions, and only a small change (3 Å) was observed in the distance (*8*). Lys-61 is located far from Cys-374 on actin, and therefore the possibility that a large-scale movement of Tm as predicted by the steric blocking theory does not produce any net change in the transfer efficiency is very small. Cys-190 of Tm is located close to the Tn-binding site, so the possibility remains that the labeled region may be not so sensitive to the movement of Tm on the thin filament. In the present study, the probe was attached to a new site of mTm (Cys-87) which is located far from Cys-190 and also from the Tn-binding site. On the other hand, many residues on actin were labeled with the fluorescence energy acceptors, which are dispersed on the outer domain of actin in the thin filament [see Fig. 5 in our previous report (*16*)]. However, in this case, no significant change was observed in the distances between

TABLE I. **Distances between probes attached to Tm and actin in the reconstituted thin filament in the presence and absence of Ca^{2+}.**

Donor site (Tm)	Acceptor site (Actin)	R_0 (2/3) (Å)	Efficiency (+Ca/−Ca)	R(2/3) (Å) (+Ca/−Ca)
Cys-87 of mTm	Nucleotide	41.4	0.72	35.2
	Gln-41	47.2	0.63	43.2
	Lys-61	47.1	0.42/0.49	49.7/47.4
	Cys-374	40.0	0.32	45.4
Cys-190 of Tm	Nucleotide	38.0	0.32	43.1
	Gln-41	43.0	0.25	51.6

probes on Tm and actin upon Ca^{2+} binding to Tn, although a small change in the distance between Lys-61 of actin and Cys-87 of Tm was observed. In both cases of Cys-190 and Cys-87 of Tm, the distance between Lys-61 of actin and the probe on Tm changed slightly depending the concentration of Ca^{2+} ions, which may indicate that the region around Lys-61 undergoes some conformational change during inhibition or activation. This is in accordance with the previous report that Lys-61 is important for the calcium-mediated regulation of the actin-myosin interaction (*34*). Bonafe *et al.* (*35*) reported that Tm affects the structure of actin subdomain 2 (segment 48-67) even in the presence of S1 bound in the rigor complex.

The involvement of myosin cross-bridges in thin filament regulation was first suggested by Bremel and Weber (*36*). They showed that at high molar ratios of S1 to actin, the ATPase activity of acto-S1 can be potentiated so that it is higher than the ATPase activity of acto-S1 in the absence of Tn-Tm. Lehrer and Morris (*37*) showed that at very low S1 concentrations, Tm greatly inhibits acto-S1 ATPase activity even in the presence of Tn and Ca^{2+}. Then, the effects of S1 (molar ratio of S1 to actin=1/3) on the transfer efficiency between probes attached to Tm and actin on the reconstituted thin filament were studied in the presence and absence of Ca^{2+} ions, but no significant effect on the transfer efficiency was observed. It seems that the activation of the thin filament by S1 binding is not accompanied by Tm movement on the actin filament. Therefore, the present results do not support the notion of Tm movement on the skeletal muscle thin filament as proposed in the steric blocking theory.

FRET measurements showed that TnI detaches from the outer domain of actin on the thin filament after Ca^{2+} binding to TnC (*8, 16, 38, 39*) and that the time scale of this movement (*39*) is well correlated with that of the conformational change of thin filament after stimulation observed by Kress *et al.* (*40*) using time-resolved X-ray diffraction of frog muscle. However, Kress *et al.* analyzed their data by assuming that a single Tm molecule, instead of Tn, will change position in an all-or-none fashion. Three-dimensional electron microscopic studies of reconstituted thin filaments (*41, 42*) have suggested that in the presence of Ca^{2+}, Tm binds to the inner domain of actin, which corresponds to subdomains 3 and 4. Using the method of site-directed mutagenesis, Saeki *et al.* (*43*) identified residues 228-232 and 241 on actin as the Tm-binding sites, which are located on subdomain 4. On the other hand, the S1-binding sites on actin are located on subdomains 1 and 2 [for review: see dos Remedios and Moens (*44*)]. Therefore, Tm has to move to the outer domain in order to inhibit sterically the actomyosin interaction, which will cause a large change (more than 10 Å) in the distance between the probes on Tm and actin used in FRET measurements [see Fig. 5 in our previous paper (*16*)]. However, FRET measurements did not detect such a large movement of Tm.

If Tm does not move on the thin filament, how does the signal for binding of Ca^{2+} propagate along the thin filament? Tm covers seven actin monomers along the two-start helix, but TnI interacts with one (or two) actin monomer. How does the TnI movement switch on or off the state of actin monomers which are covered by Tm? We showed that during inhibition, the C-terminal and inhibitory domains of TnI move towards the outer domain of actin (*16*). These

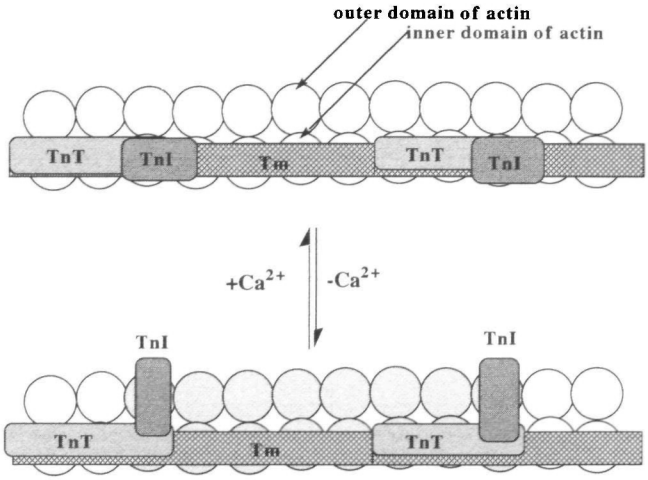

Fig. 6. **A schematic model of troponin and tropomyosin along the long-pitch helix of the actin filament in the presence and absence of Ca^{2+}.** One actin molecule is illustrated with two circles which represent the outer and inner domains of actin. The open circles represent the "ON" state and shaded circles indicate the "OFF" state of actin. One tropomyosin covers the inner domains of 7 actin monomers along the long-pitch helix. When two neighbouring TnI subunits along Tm crosslink the outer domains of two actin monomers, the eight actin monomers covered by two TnI and Tm are switched to the OFF State.

results suggest that, in the absence of Ca^{2+}, Tn cross-links the outer domain of one actin monomer with Tm which covers seven actin monomers in F-actin. The cross-linkings of the inner and outer domains of actin by Tm-Tn may cause a considerable distortion of the actin helix and/or a significant immobilization of internal motion of the outer domain of actin monomers which are located between neighboring two cross-linkings along the two-start helix. A schematic model of troponin and tropomyosin along the long-pitch helix of the actin filament in the presence and absence of Ca^{2+} is illustrated in Fig. 6. In this model, Tm does not compete with the binding to actin with S1, in accordance with experiment. For a more complete understanding of the regulation of skeletal muscle contraction, further experiments based on the structure of thin filament are necessary.

We thank the Food Research and Development Laboratories of Ajinomoto Co. for the generous gift of microbial transglutaminase, and Prof. Ikunobu Muramatsu at Fukui Medical University for kindly providing rabbit hearts.

REFERENCES

1. Ebashi, S., Endo, M., and Ohtsuki, I. (1969) Control of muscle contraction. *Q. Rev. Biophys.* **2**, 351-384
2. Huxley, H.E. (1972) Structural changes in the actin and myosin containing filaments during contraction. *Cold Spring Harbor Symp. Quant. Biol.* **37**, 361-376
3. Haselgrove, J. (1972) X-ray evidence for a conformational change in the actin containing filaments of vertebrate striated muscle. *Cold Spring Harbor Symp. Quant. Biol.* **37**, 341-352
4. Lorenz, M., Popp, D., and Holmes, K.C. (1993) Refinement of the F-actin model against X-ray fiber diffraction data by the use of a directed mutation algorithm. *J. Mol. Biol.* **234**, 826-836
5. Holmes, K.C. (1995) The actomyosin interaction and its control by tropomyosin. *Biophys. J.* **68**, 2s-7s

6. Lehman, W., Vibert, P., Uman, P., and Craig, R. (1995) Steric-blocking by tropomyosin visualized in relaxed vertebrate muscle thin filaments. *J. Mol. Biol.* **251**, 191-196
7. Tao, T., Lamkin, M., and Lehrer, S.S. (1983) Excitation energy transfer studies of the proximity between tropomyosin and actin in reconstituted skeletal muscle thin filaments. *Biochemistry* **22**, 3059-3066
8. Miki, M. (1990) Resonance energy transfer between points in a reconstituted skeletal muscle thin filament: A conformational change of the thin filament in response to a change in Ca^{2+} concentration. *Eur. J. Biochem.* **187**, 155-162
9. Monteiro, P.B., Lataro, C., Ferro, J.A., and Reinach, F.C. (1994) Functional α-tropomyosin produced in *Escherichia coli*. *J. Biol. Chem.* **269**, 10461-10466
10. Hiratsuka, T. and Uchida, K. (1973) Preparation and properties of 2′(or 3′)-*O*-(2,4,6-trinitrophenyl)adenosine 5′-triphosphate, an analog of adenosine triphosphate. *Biochim. Biophys. Acta* **320**, 635-647
11. Lewis, W. and Smillie, L.B. (1980) The amino acid sequence of rabbit cardiac tropomyosin. *J. Biol. Chem.* **255**, 6854-6859
12. Nonaka, M., Sakamoto, H., Toiguchi, S., Kawajiri, H., Soeda, T., and Motoki, M. (1992) Sodium caseinate and skim milk gels formed by incubation with microbial transglutaminase. *J. Food Sci.* **57**, 1214-1241
13. Kim, E., Motoki, M., Seguro, K., Muhlrad, A., and Reisler, E. (1995) Conformational changes in subdomain 2 of G-actin: Fluorescence probing by dansyl ethylenediamine attached to Gln-41. *Biophys. J.* **69**, 2024-2032
14. Kluwe, L., Maeda, K., Miegel, A., Fujita-Becker, S., Maéda, Y., Talbo, G., Houthaeve, T., and Kellner, R. (1995) Rabbit skeletal muscle $\alpha\alpha$-tropomyosin expressed in baculovirus-infected insect cells possesses the authentic N-terminus structure and functions. *J. Muscle Res. Cell Motil.* **16**, 103-110
15. Miegel, A., Sano, K., Yamamoto, K., Maeda, K., Maéda, Y., Taniguchi, H., Yao, M., and Wakatsuki, S. (1996) Production and crystallization of lobster muscle tropomyosin expressed in Sf9 cells. *FEBS Lett.* **394**, 201-205
16. Miki, M., Kobayashi, T., Kimura, H., Hagiwara, A., Hai, H., and Maéda, Y. (1998) Ca^{2+}-induced distance change between points on actin and troponin in skeletal muscle thin filaments estimated by fluorescence energy transfer spectroscopy. *J. Biochem.* **123**, 324-331
17. Lorand, L., Parameswaran, K.N., Velasco, P.T., Hsu, L.K.-H., and Siefring, G.E., Jr. (1983) New colored and fluorescent amine substrates for activated fibrin stabilizing factor (Factor XIIIa) and for transglutaminase. *Anal. Biochem.* **131**, 419-425
18. Bernhardt, R., Ngoc Dao, N.T., Stiel, H., Schwarze, W., Friedrich, J., Janig, G.R., and Ruckpaul, K. (1983) Modification of cytochrome P-450 with fluorescein isothiocyanate. *Biochim. Biophys. Acta* **745**, 140-148
19. Hudson, E.N. and Weber, G. (1973) Synthesis and characterization of two fluorescent sulfhydryl reagents. *Biochemistry* **12**, 4154-4161
20. Miki, M. (1987) The recovery of the polymerizability of Lys-61-labelled actin by the addition of phalloidin. *Eur. J. Biochem.* **164**, 229-235
21. Stryer, L. (1978) Fluorescence energy transfer as a spectroscopic ruler. *Annu. Rev. Biochem.* **47**, 819-846
22. Lakowicz, J.R. (1983) *Principles of Fluorescence Spectroscopy*, Plenum Press, New York
23. Dale, R.E., Eisinger, J., and Blumberg, W.E. (1979) Orientational freedom of molecular probes: Orientation factor in intramolecular energy transfer. *Biophys. J.* **26**, 161-194
24. Laemmli, U.K. (1970) Cleavage of structural proteins during the assembly of the head of bacteriophage T4. *Nature* **227**, 680-685
25. Tausky, H.H. and Shorr, E. (1953) A microcolorimetric method for the determination of inorganic phosphorus. *J. Biol. Chem.* **202**, 675-685
26. Lehrer, S.S. and Ishii, Y. (1988) Fluorescence properties of acrylodan-labeled tropomyosin and tropomyosin-actin: Evidence for myosin subfragment 1 induced changes in geometry between tropomyosin and actin. *Biochemistry* **27**, 5899-5906
27. Zot, H.G. and Potter, J.D. (1987) Structural aspects of troponin-tropomyosin regulation of skeletal muscle contraction. *Annu. Rev. Biophys. Biophys. Chem.* **16**, 535-559
28. Mabuchi, K. (1996) Electron microscopic study of tropomyosin binding to actin filaments reveals tethered molecules representing weak binding. *J. Struct. Biol.* **116**, 278-289
29. Fujime, S. and Ishiwata, S. (1971) Dynamic study of F-actin by quasielastic scattering of laser light. *J. Mol. Biol.* **62**, 251-265
30. Kasprzak, A.A., Takashi, R., and Morales, M.F. (1988) Orientation of the actin monomer in the F-actin filament: Radial coordinate of glutamine-41 and effect of myosin subfragment-1 binding on the monomer orientation. *Biochemistry* **27**, 4512-4522
31. Chen, R.F. and Bowman, R.L. (1965) Fluorescence polarization: Measurement with ultraviolet-polarizing filters in a spectrophotofluorometer. *Science* **147**, 729-732
32. Miki, M., O'Donoghue, S.I., and dos Remedios, C.G. (1992) Structure of actin observed by fluorescence resonance energy transfer spectroscopy. *J. Muscle Res. Cell Motil.* **13**, 132-145
33. dos Remedios, C.G. and Moens, P.D.J. (1995) Fluorescence resonance energy transfer spectroscopy is a reliable "ruler" for measuring structural changes in proteins: Dispelling the problem of the unknown orientation factor. *J. Struct. Biol.* **115**, 175-185
34. Miki, M. (1989) Interaction of Lys-61 labeled actin with myosin subfragment 1 and the regulatory proteins. *J. Biochem.* **106**, 651-655
35. Bonafe, N., Mathieu, M., Kassab, R., and Chaussepied, P. (1994) Tropomyosin inhibits the glutaraldehyde-induced cross-link between the central 48-kDa fragment of myosin head and segment 48-67 in actin subdomain 2. *Biochemistry* **33**, 2594-2603
36. Bremel, R.D. and Weber, A. (1972) Cooperation within actin filament in vertebrate skeletal muscle. *Nature* **238**, 97-101
37. Lehrer, S.S. and Morris, E.P. (1982) Dual effects of tropomyosin and troponin-tropomyosin on actomyosin subfragment 1 ATPase. *J. Biol. Chem.* **257**, 8073-8080
38. Tao, T., Gong, B-J., and Leavis, P.C. (1990) Calcium-induced movement of troponin-I relative to actin in skeletal muscle thin filaments. *Science* **247**, 1339-1341
39. Miki, M. and Iio, T. (1993) Kinetics of structural changes of reconstituted skeletal muscle thin filaments observed by fluorescence resonance energy transfer. *J. Biol. Chem.* **268**, 7101-7106
40. Kress, M., Huxley, H.E., Faruqi, A.R., and Hendrix, J. (1986) Structural changes during activation of frog muscle studied by time-resolved X-ray diffraction. *J. Mol. Biol.* **188**, 325-342
41. Milligan, R.A., Whittaker, M., and Safer, D. (1990) Molecular structure of F-actin and location of surface binding sites. *Nature* **348**, 217-221
42. Ishikawa, T. and Wakabayashi, T. (1994) Calcium induced change in three-dimensional structure of thin filaments of rabbit skeletal muscle as revealed by cryo-electron microscopy. *Biochem. Biophys. Res. Commun.* **203**, 951-958
43. Saeki, K., Sutoh, K., and Wakabayashi, T. (1996) Tropomyosin-binding site(s) on the *Dictyostelium* actin surface as identified by site-directed mutagenesis. *Biochemistry* **35**, 14465-14472
44. dos Remedios, C.G. and Moens, P.D.J. (1995) Actin and the actomyosin interface: a review. *Biochim. Biophys. Acta* **1228**, 99-124